Fish and Shellfish Immunology 86 (2019) 311–318

Contents lists available at ScienceDirect

Fish and Shellfish Immunology

journal homepage: www.elsevier.com/locate/fsi

Short communication

# Transcriptome analysis of differential expressed genes in hepatopancreas of *Procambarus clarkii* challenged with peptidoglycan

Xiao-Hua Chu[a,b,1], Ting-Ting Yang[a,c,1], Yu Liu[a,c,1], Liang Hong[d,1], Ting Jiao[a], Xun Meng[a], Dai-Zhen Zhang[a], Jia-Lian Wang[a], Bo-Ping Tang[a], Chun-Lin Zhou[a], Qiu-Ning Liu[a,***], Wei-Wei Zhang[d,*], Wen-Fei He[b,**]

[a] *Jiangsu Key Laboratory for Bioresources of Saline Soils, Jiangsu Synthetic Innovation Center for Coastal Bio-agriculture, Jiangsu Provincial Key Laboratory of Coastal Wetland Bioresources and Environmental Protection, School of Ocean and Biological Engineering, Yancheng Teachers University, Yancheng, 224007, PR China*
[b] *School of Pharmaceutical Sciences, Wenzhou Medical University, Wenzhou, 325035, PR China*
[c] *College of Biotechnology and Pharmaceutical Engineering, Nanjing University of Technology, Nanjing, 210009, PR China*
[d] *Department of Infectious Disease, Ruian People's Hospital, Wenzhou, Zhejiang, 325200, PR China*

ARTICLE INFO

*Keywords:*
*Procambarus clarkii*
Peptidoglycan (PGN)
Hepatopancreas
Immune system
Transcriptome

ABSTRACT

*Procambarus clarkii* is one of the most economically important species in Chinese aquaculture, and is widely cultured. Infection of *P. clarkii* populations with bacterial pathogens causes high mortality and great economic loss, therefore disease control is of significant economic importance. *P. clarkii* is a model system for studying immune responses in invertebrates, and its immune system consists solely of the innate response. In the present study, we examined gene expression related to immune function in *P. clarkii* in response to pathogen challenge. The transcriptome of hepatopancreas tissue from *P. clarkii* challenged with peptidoclycan (PGN) was analyzed and compared to control specimens. After assembly and annotation, 48,661 unigenes were identified with an average length of 671.54 bp. A total of 2533 differentially expressed genes (DEGs) were obtained, including 765 significantly up-regulated unigenes and 1757 significantly down-regulated unigenes. Gene ontology (GO) analysis demonstrated 19 biological process subcategories, 16 cellular component subcategories, and 17 molecular function subcategories that were enriched among these DEGs. Enrichment analysis using the Kyoto Encyclopedia of Genes and Genomes (KEGG) database revealed enrichment among immune responses pathways. Taken together, this study not only enriches the existing *P. clarkii* transcriptome database, but also elucidates immune responses of crayfish that are activated in response to PGN challenge.

## 1. Introduction

The red swamp crayfish, *Procambarus clarkii*, is a freshwater crayfish species native to Mexico and North America that was introduced into China during the 1930s [1]. The red swamp crayfish is now widely cultured in China because of its good taste, strong ability to adapt to complex environments, and its commercial value; due to these advantages, the red swamp crayfish has one of the most economically important cultured aquatic products in China [2]. Additionally, the red swamp crayfish serves as a model organism to study aquaculture pathogen infections. Pathogen infections are damaging to the sustainability of the expanding aquaculture industry. In this study, we analyzed the transcriptomes of hepatopancreas tissue in red swamp crayfish challenged with peptidoglycan (PGN). PGNs, major components of Gram-positive bacterial cell walls, induce immune activities in metazoans and plants [3,4]. PGN serves a structural role in the bacterial cell wall, giving structural strength, as well as counteracting the osmotic pressure of the cytoplasm [5]. A large amount of survey revealed that PGN may play a vital role to regulate the immune function. The PGN can promote phagocytic cell function and facilitate the release of cytokines and nitric oxide and other immune mediators. In this way, PGN plays a key role in the anti-infection and anti-tumor immune [6]. In order to identify mechanisms activated in *P. clarkii* in response to pathogen infection, a cDNA library was constructed to evaluate

* Corresponding author.
** Corresponding author.
*** Corresponding author.
*E-mail addresses:* liuqn@yctu.edu.cn (Q.-N. Liu), 461357478@qq.com (W.-W. Zhang), wenfei509@163.com (W.-F. He).
[1] These authors contributed equally to this work.

https://doi.org/10.1016/j.fsi.2018.11.048
Received 30 September 2018; Received in revised form 12 November 2018; Accepted 17 November 2018
Available online 19 November 2018
1050-4648/ 

**Table 1**
List of the quality of transcriptomic sequencing data of *P. clarkii*.

| sample | Clean reads | Clean bases | GC(%) | Q30(%) |
|---|---|---|---|---|
| PBS | 22,067,581 | 6,589,701,420 | 53.79% | 92.37% |
| PGN | 30,270,827 | 9,046,226,824 | 47.43% | 93.06% |

**Table 2**
Summary of de novo assembly of transcriptomic profiles of *P. clarkii*.

| Length range | Transcript | Unigene |
|---|---|---|
| 200–300 | 18,969(31.65%) | 17,882(36.75%) |
| 300–500 | 14,772(24.65%) | 12,616(25.93%) |
| 500–1000 | 12,947(21.60%) | 9708(19.95%) |
| 1000–2000 | 8379(13.98%) | 5557(11.42%) |
| 2000 + | 4868(8.12%) | 2898(5.96%) |
| Total Number | 59,935 | 48,661 |
| Total Length | 46,699,941 | 32,677,798 |
| N50 Length | 1292 | 1035 |
| Mean Length | 779.18 | 671.54 |

**Table 3**
Statistical comparison between sequenced data and assembly results.

| ID | Clean Reads | Mapped Reads | Mapped Ratio |
|---|---|---|---|
| PBS | 22,067,581 | 16,492,695 | 74.74% |
| PGN | 30,270,827 | 24,162,368 | 79.82% |

differentially expressed genes (DEGs) in hepatopancreas of red swamp crayfish challenged with PGN compared to a phosphate-buffered saline (PBS) control treatment.

*Procambarus clarkii* is an important cambarid species of freshwater crayfish. The immune system of invertebrate animals is composed only of an innate immune component, and invertebrate immune systems lacks adaptive immune systems [7,8]. The innate immune system is of vital importance in defense against virus and bacterial pathogens [9], and detects invasion of microbial pathogens through Toll-like receptors (TLRs) [10]. Recognition of pathogens by TLRs triggers specific gene expression responses. Innate immune responses and antigen-specific acquired immunity are controlled by TLR-responsive gene products [11].

RNA-sequencing (RNA-seq) uses deep-sequencing technologies to produce transcriptome profiles. RNA-seq provides a much more accurate measurement of levels of specific transcripts than other technologies, and is a reliable high-throughput method for transcriptome analysis [12]. This technology brings new methods and novel insights to transcriptomic experiments. RNA-seq has previously been applied to work out the complexity of the *P. clarkii* transcriptome [13]. In the present study, cDNA libraries were established from hepatopancreas tissue of two groups of *P. clarkii*, one injected with PGN and the other exposed to PBS. The DEGs were analyzed and categorized into different functional sets. The immune-related DEGs were identified and analyzed using GO (Gene ontology) and KEGG (Kyoto Encyclopedia of Genes and Genomes) pathway enrichment analysis. The results of this study clarify the gene expression responses of *P. clarkii* to pathogen challenge, and provide crucial information for future studies into the *P. clarkii* immune system.

## 2. Materials and methods

### 2.1. Experimental PGN infection and hepatopancreas tissue collection

*P. clarkii* were purchased from the Yancheng market in Yancheng, Jiangsu Province, China. Similarly sized (20–25 g) specimens were chosen and placed in an ultraviolet radiation sterilization circulating water temperature-controlled aquaculture system for several weeks [14]. Qualified samples were stabilized for one week [15,16]. All crayfish in the experimental group (three individuals) and three crayfish in the control group received an injection of 20 μL PGN (1 mg/ml) or 20 μL PBS, respectively. Twenty-four hours post-injection, the hepatopancreas tissues were collected and stored at −80 °C.

### 2.2. RNA extraction, library construction, and RNA sequencing

Total RNA was extracted using TRIzol reagent (Sangon, China), in accordance with the manufacturer's instructions. After extraction, the RNA concentration was measured by a Nanodrop spectrophotometer, and the purity and completeness of extracted RNA were checked using Qubit 2.0 and an Agilent 2100 instrument, respectively.

After confirmation of sample quality, cDNA libraries were constructed. Briefly, mRNA was enriched by incubation with magnetic beads coupled to oligo (dt) [17]. Fragmentation buffer was then added to randomly digest the mRNA into pieces. Subsequently, first-strand cDNA synthesis was performed using random hexamers. and buffer, dNTPs, RNase H, and DNA polymerase I. Library fragments were purified with AMPure XP beads to select cDNA fragments of 150–200 bp in

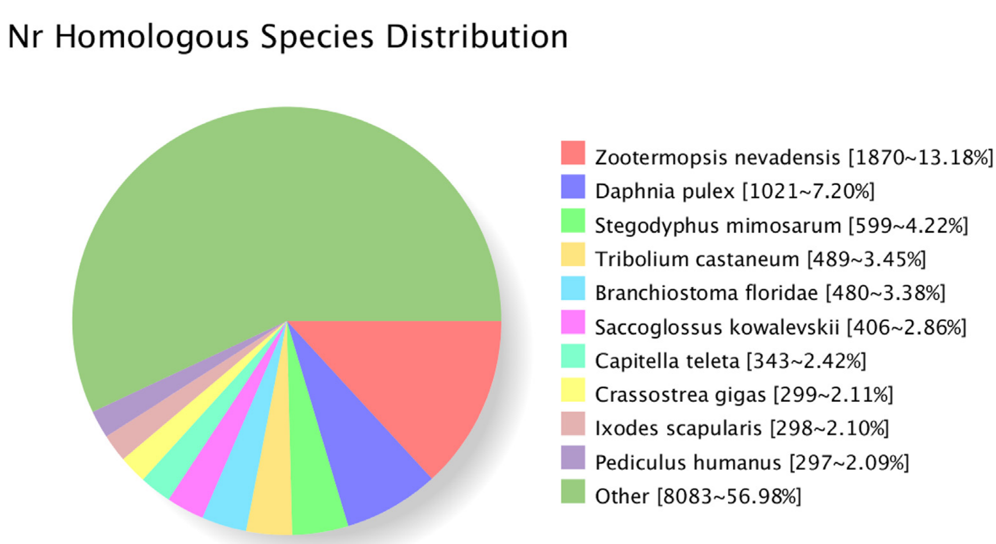


**Fig. 1.** Nr homologous species distribution of best hits for each unigene

**Table 4**
Distribution of DEGs in different functional databases.

| Annotated databases | Annotation number | Percentage(%) | 300 ≤ length ≤ 1000 | length ≥ 1000 |
|---|---|---|---|---|
| COG_annotation | 5258 | 30.80 | 1848 | 2156 |
| GO_annotation | 7294 | 42.73 | 2925 | 2502 |
| KEGG_annotation | 8161 | 47.81 | 3209 | 3180 |
| KOG_annotation | 11672 | 68.11 | 4462 | 4275 |
| Pfam_annotation | 12086 | 70.80 | 4714 | 4757 |
| Swissprot_annotation | 8643 | 50.63 | 3293 | 3569 |
| EggNOG_annotation | 15422 | 90.35 | 6093 | 4947 |
| NR_annotation | 14209 | 83.24 | 5932 | 5080 |
| All_annotation | 17070 | 100 | 6811 | 5392 |

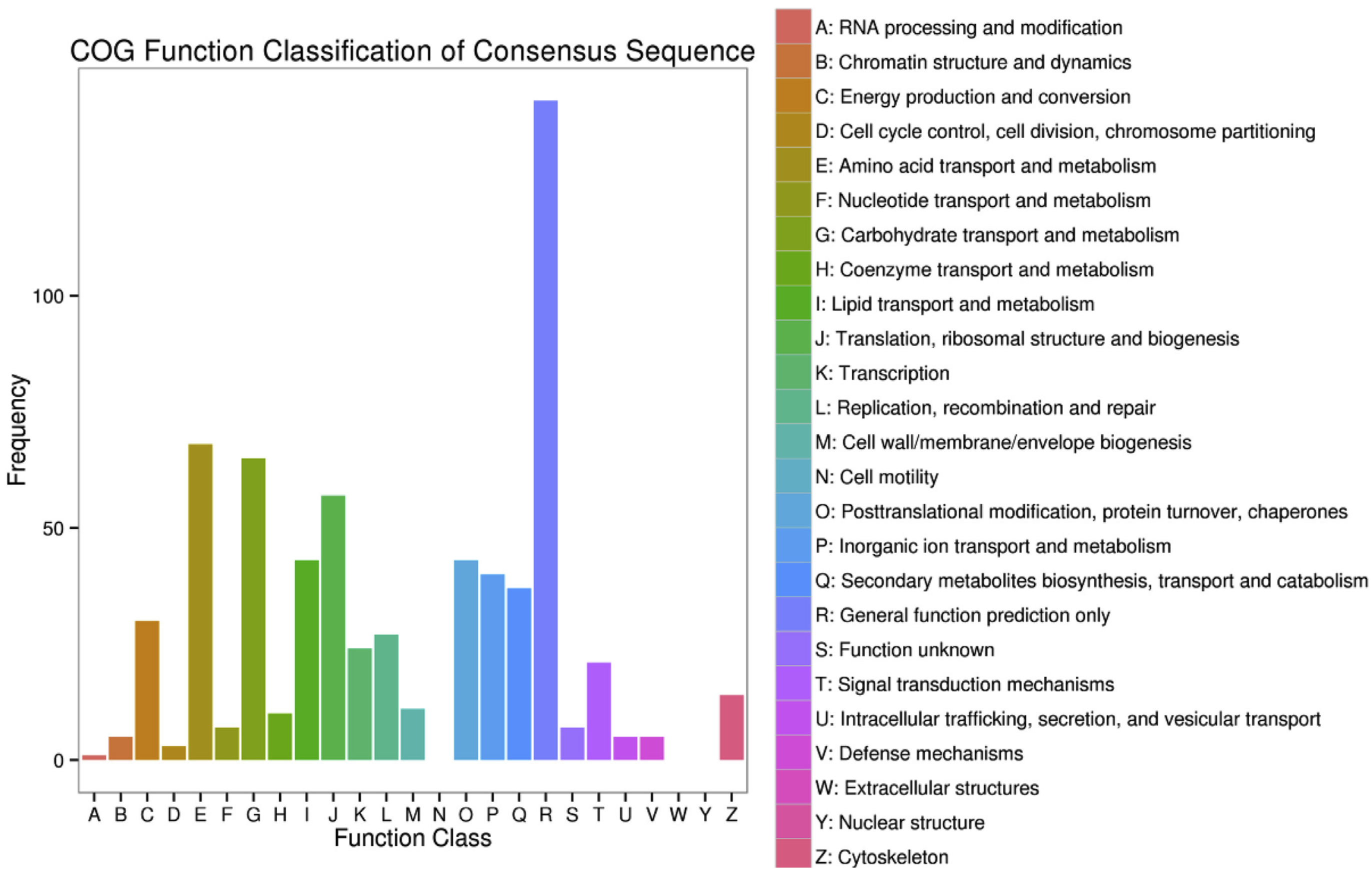


**Fig. 2.** COG function classification of consensus sequence. The X-axis represents names of 25 groups, the Y-axis corresponds to the number of genes in the group.

length. Finally, suitable adaptor-ligated fragments were enriched by PCR to obtain the final cDNA library.

After the construction of the cDNA libraries, the concentration and the insert size were measured by Qubit 2.0 and an Agilent 2100 instrument, respectively. The effective concentration of the cDNA libraries was accurately quantified using qRT-PCR to ensure the quality. The libraries of PBS- and PGN- infection were then sequenced on an Illumina Hiseq instrument.

### 2.3. Sequencing data processing and assembly

Raw sequencing data was filtered to obtain clean, high quality data by removing raw data with adapter and low-quality reads. Clean data was then concatenated based on the reference sequence. Subsequently, the sequences were assembled to form unigenes. At the same time, Q20, Q30, GC-content, and sequence duplication levels of the clean reads were calculated.

The cDNA library from the PBS- and PGN-treated groups were sequenced with an Illumina Hiseq 2500 instrument. A large amount of high-quality reads were obtained, which is necessary to ensure the accuracy of sequence assembly and subsequent analyses. The quality scores of most of the reads in PGN-treated groups were over the Q30 level, indicating that the data are reliable for further analysis. Trinity software was used for the de novo assembly of the RNA-Seq data.

### 2.4. Functional annotation and classification of unigenes

Unigenes were aligned against the NCBI non-redundant protein database NR (http://www.ncbi.nlm.nih.gov), Swiss-prot (http://www.uniprot.org), the Clusters of Orthologous Group of Proteins database (COG, http://www.ncbi.nlm.nih.gov/COG/), and the Kyoto Encyclopedia of Genes and Genomes (KEGG, http://www.genome.jp/kegg) by BLASTx with E-value of less than $10^{-5}$ [18–20]. Unigenes were defined according to top hits against known sequence retrieved from the BLAST search [12,21]. The NR database is a redundant protein database containing information from Swiss-Prot, PIR, PRF, and PDB [22]. The Swiss-Prot database is maintained by EBI, and contains curated protein annotation data. The Clusters of Orthologous Group is a

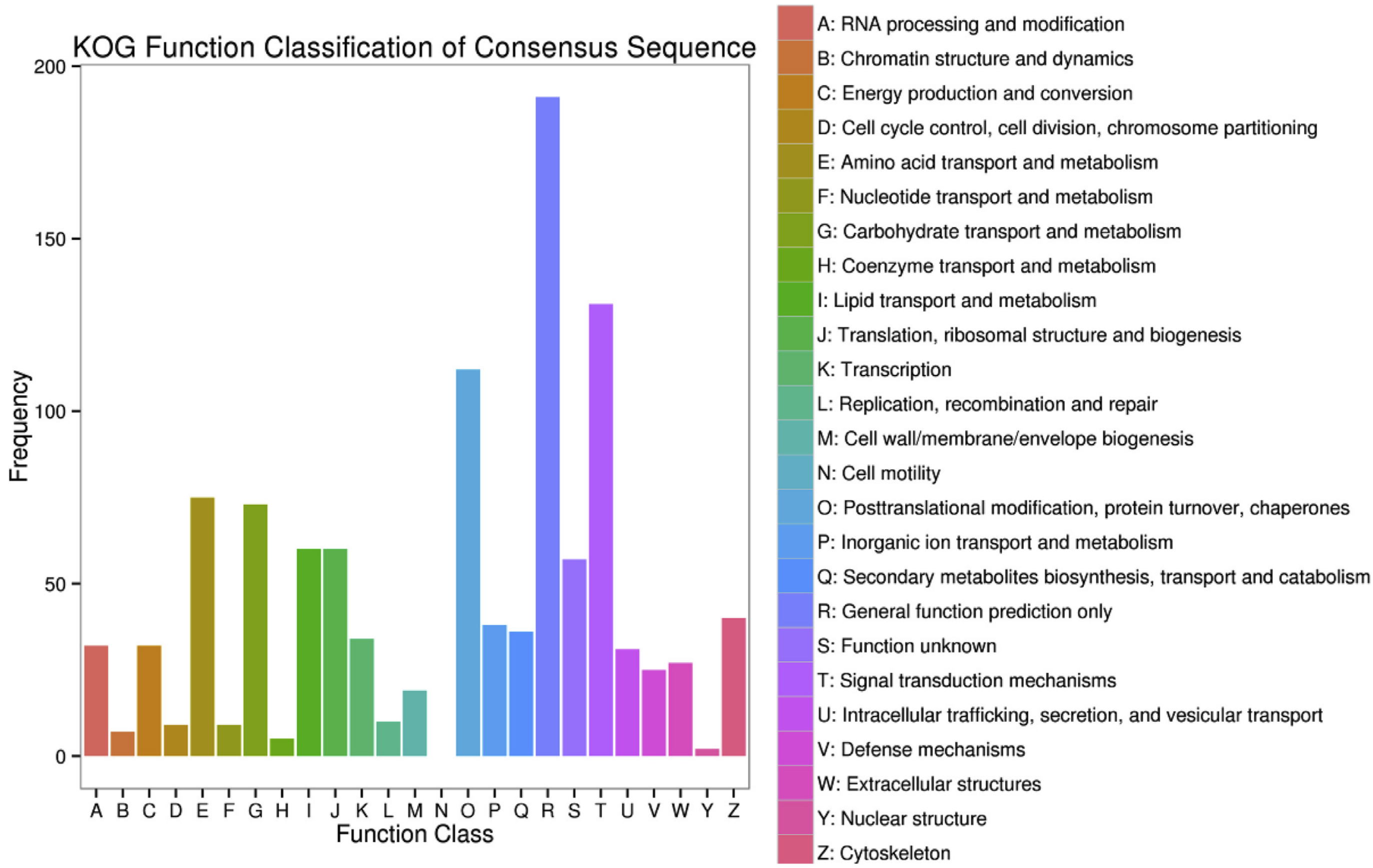


**Fig. 3.** Classification of the unigenes annotated in KOG (26 groups). The X-axis represents the names of the 26 groups, and the Y-axis corresponds to the percentage of the number of genes in the group accounting for the total number of annotated genes.

database used to obtain detailed functional predictions and classifications of unigenes [23]. The NOG database contains functional description and classification information of homologous proteins, combining COG, KOG, and additional databases, and covers more protein sequences than the COG and KOG databases alone, including 5228 viral proteins.

## 3. Results and discussion

### 3.1. Assembly and splicing

A total of 22,067,581 clean reads were obtained from the control (PBS-treated) samples and 30,270,827 clean reads from the PGN-treated samples; clean base numbers for these groups were 6,589,701,420 and 9,046,226,824, respectively. Q30 values for the two groups were about 92.37% and 93.06%, respectively. The G + C content of the sequences was approximately 53.79% in the PBS-treated samples and 47.43% in PGN-treated samples (Table 1). 59,935 transcripts were generated with a mean length of 779.18 bp and an N50 length of 1292 bp, as assessed by Trinity software. 48,661 unigenes were identified with an average length of 671.54 bp and an N50 length of 1035 bp. Among these unigenes, 30,498 (62.68%) were in the range of 200–500 bp, 9708 (19.95%) in the 500–1000 bp range, 5557 (11.42%) in the 1–2 kbp range, and 2898 (5.96%) unigenes were longer than 2 kbp (Table 2). Additionally, 74.74% and 79.82% were mapped to the genome in the PBS control group and the PGN infection group, respectively (Table 3). These results indicate the high quality of the data, and demonstrate that the unigenes are suitable for further analysis. The raw reads of RNA-Seq were deposited in the Sequence Read Archive (SRA) database of NCBI with the accession numbers of SRR8151935 and SRR8151934. In addition, 1870 (13.18%), 1021 (7.20%), and 599 (4.22%) unigenes were homologous to protein coding sequences from *Zootermopsis nevodensis*, *Daphnia pulex,* and *Stegodyphus mimosarum*, respectively (Fig. 1).

### 3.2. Functional annotation and classification

Eight databases were used to annotate the unigenes to obtaining comprehensive gene function information, including COG, GO, KEGG, KOG, Swissprot, eggNOG, NR, and Pfam. In total, 17,070 unigenes were annotated as follows: 5285 in COG (30.80%), 7294 in GO (42.73%), 8186 in KEGG (47.81%), 11,672 in KOG (68.11%), 12,086 in Pfam (70.80%), 8643 in Swiss-prot (50.63%), 15,422 in eggNOG (90.35%), and 14,209 in NR (83.24%) (Table 4) [24].

### 3.3. GO, COG and KOG classification of transcriptome sequences

The functions of the target unigenes were classified by the GO and KEGG databases [25–27]. GO database is a functional classification system of genes that follows international standards. It offers a standard, dynamically updated database to describe gene functions in organisms [28]. The GO database describes the molecular function of the gene products, the cellular environment, and biological processes that genes are involved in Ref. [20]. The GO database is applicable to all species. In total, 7294 unigenes were classified into three main categories including “cellular component”, “molecular function”, and “biological process” and 52 additional subcategories. Within the “cellular component” category, most unigenes were assigned into the “cell” subcategory (2427, 22.17%). In the “molecular function” category, many unigenes were in the “catalytic activity” (4024, 44.04%) and “binding” subcategories (3552, 38.87%). The majority of unigenes in the category of “biological process” were involved in the “metabolic

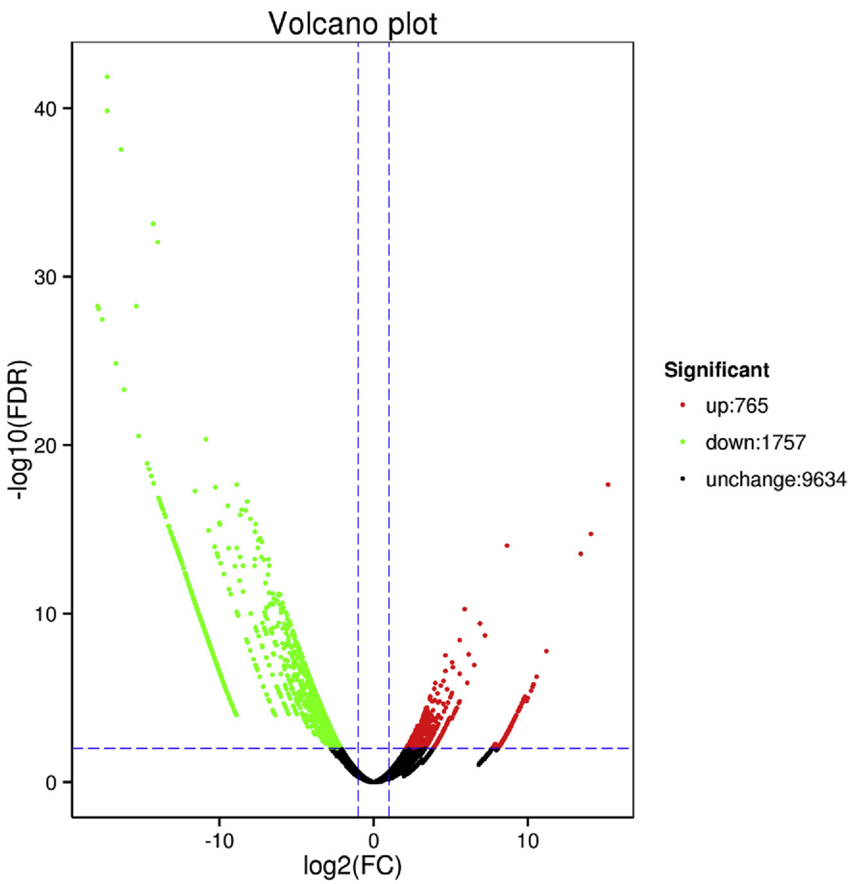


**Fig. 4.** Volcano plot of DEGs identified between the PGN and PBS groups. The red dots represent significantly up-regulated unigenes. The green dots represent significantly down-regulated unigenes. The black dots represent unigenes that did not have any significant differential expression. (For interpretation of the references to colour in this figure legend, the reader is referred to the Web version of this article.)

**Table 5**
The number of DEGs analyzed by different functional databases.

| DEG set | Annotated | COG | GO | KEGG | KOG | Pfam | Swiss-Prot | eggNOG | Nr |
|---|---|---|---|---|---|---|---|---|---|
| PBS vs PGN | 1522 | 506 | 634 | 696 | 991 | 1293 | 907 | 1313 | 1380 |

process" (4918, 26.36%) and "cellular process" (3865, 20.71%) subcategory. In the GO classification, 69 unigenes were assigned to "immune system process" and 885 unigenes were annotated to "response to stimulus". These results suggest that the processes induced by PGN are related to immune responses. COG database is used to acquire detailed functional predictions and classifications of unigenes. A total of 5258 unigenes were classified into 25 categories; "General function prediction only" is the largest group (Fig. 2). In the KOG classification, 11,672 unigenes were classified into 25 categories. Among these groups, "General function prediction only" is the largest group (Fig. 3).

### 3.4. Identification and analysis of DEGs

All of the unigenes were analyzed with the q-value threshold restricted to $q < 0.005$ [24,30], $|\log_2 \text{(foldchange)}| \geq 2$. We identified 2522 significant DEGs between the PGN-challenged and PBS control groups, including 765 up-regulated and 1757 down-regulated unigenes (Fig. 4). The number of DEGs represented and characterized in the different functional databases are as follows: 506 in COG, 634 in GO, 696 in KEGG, 991 in KOG, 1293 in Pfam, 907 in Swiss-Prot, 1313 in eggNOG, and 1380 in Nr (Table 5). In the volcano plot, the red dots represented significantly up-regulated unigenes, and the green dots represented significantly down-regulated unigenes. The black dots represented unigenes that were not significantly differentially expressed [29–31]. The magnitude in change in levels of up-regulated DEGs was significantly lower than the magnitude in change of levels of down-regulated DEGs.

### 3.5. Enrichment analysis of DEGs

In the GO database, all DEGs were classified into three categories by topGO, including "biological process" (BP), "cellular component" (CC), and "molecular function" (MF) [32], composed of 19, 16, and 17 subcategories, respectively. Among the various categories of BP, the top three by frequency were "metabolic process", "cellular process", and "single-organism process". In the CC classes, "cell", "cell part", and "organelle" constituted the top three clusters by frequency. Within the MF subcategories, "catalytic activity", "binding", and "transporter activity" were the most enriched groups (Fig. 5).

GO analysis identified 177 unigenes enriched in the "Immune system process" and 2925 unigenes in the "Response to stimulus" categories. The "Immune system process" category includes eight subcategories: "Immune system process", "Regulation of defense response to virus", "Mucosal immune response", "Innate immune response", "Regulation of innate immune response", "Innate immune response in mucosa", "Immune response" and "Positive regulation of immune response". "Immune response", which contains 56 unigenes and 7 DEGs, dominates these subcategories. Within the "Response to stimulus" category, the largest subcategory was "Response to stimulus", with 1001 unigenes and 72 DEGs (Table 6).

In the present study, many genes response to the PGN stimulus strongly, such as chitinase, heat shock protein 70 (Hsp70) and

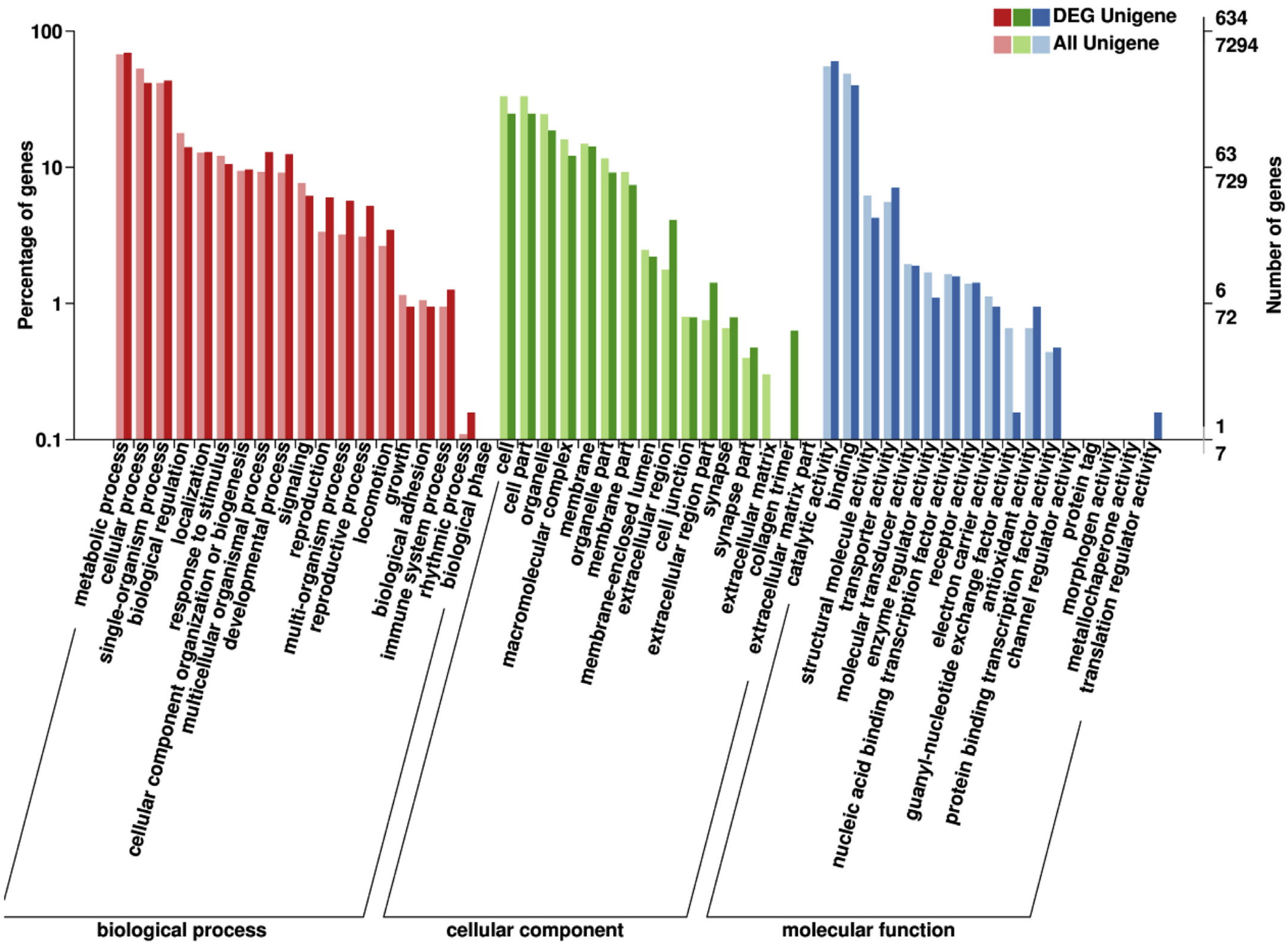


**Fig. 5.** Histogram depiction of Gene Ontology enrichment of DEGs. All the DEGs fell into three categories: "biological process" (BP), "cellular component" (CC), and "molecular function" (MF). The X-axis represents various gene functions, and the Y-axis corresponds to the number of DEGs.

**Table 6**
The number of unigenes related to the immune system enriched in different GO terms.

| GO ID | Term | Unigene | DEGs | P-value |
|---|---|---|---|---|
| GO:0002376 | immune system process | 84 | 11 | 0.23348 |
| GO:0050688 | regulation of defense response to virus | 1 | 0 | 0.56679 |
| GO:0002385 | mucosal immune response | 2 | 0 | 0.62361 |
| GO:0045087 | innate immune response | 27 | 5 | 0.32269 |
| GO:0045088 | regulation of innate immune response | 2 | 0 | 0.98829 |
| GO:0002227 | innate immune response in mucosa | 1 | 0 | 0.2409 |
| GO:0006955 | immune response | 56 | 7 | 0.51666 |
| GO:0050778 | positive regulation of immune response | 4 | 1 | 0.67022 |
| GO:0080134 | regulation of response to stress | 20 | 2 | 0.89527 |
| GO:0009968 | negative regulation of signal transduction | 51 | 4 | 0.36829 |
| GO:0033554 | cellular response to stress | 152 | 7 | 0.95479 |
| GO:0007165 | signal transduction | 601 | 33 | 0.98321 |
| GO:0009967 | positive regulation of signal transduction | 19 | 1 | 0.50876 |
| GO:0050896 | response to stimulus | 1001 | 72 | 0.96116 |
| GO:0048583 | regulation of response to stimulus | 221 | 12 | 0.73937 |
| GO:0051716 | cellular response to stimulus | 715 | 38 | 0.9998 |
| GO:0006974 | cellular response to DNA damage stimulus | 115 | 3 | 0.94912 |
| GO:0009416 | response to light stimulus | 30 | 0 | 0.79202 |

hemocyanin (HMC). Chitinases were identified from red swamp crayfish (*P. clarkii*) within |log2(fold change)| = 10.214. The transcripts of chitinases were found to be up-regulated significantly in hepatopancreas. Researches before have already indicated that chitinases are of much concern in defense against viruses [33]. Chitin, the second most important natural polymer in the world, which mainly derived from shrimp and crabs [34]. It is the main structural material in cell walls of the shell and radulae of mollusks. In the middle to late 1980s, the activation of chitin and chitin derivatives in immune responses was revealed and explored. It had been demonstrated that chitin was a size-dependent pathogen-associated molecular pattern, activating toll-like receptor 2 (TLR2) in an innate immunity pathway [35]. Hsp70 is of vital importance to resist environmental stresses and to stimulate innate immune system. The obviously high levels of Hsp70 transcript were in hepatopancreas according to the research before [36]. Hsps play an essential role in protecting cells by folding and translocating nascent proteins and are preserved throughout evolution extensively. Hsp70 induces and participates in protein folding and apoptosis. What's more, it is involved in specific immune responses and in innate immune responses which works as regulators [37]. In hepatopancreas of *P. clarkii* challenged with PGN, Hsp70 was found to be significantly up-regulated within |log2(fold change)| = 8.273. HMCs, versatile macromolecules, contain strong immunogenic and immunomodulatory properties [38]. It has the function of multifunctional non-specific innate immune defense in shrimp [39], Which was found to be up-regulated with the value |log2(fold change)| = 6.900.

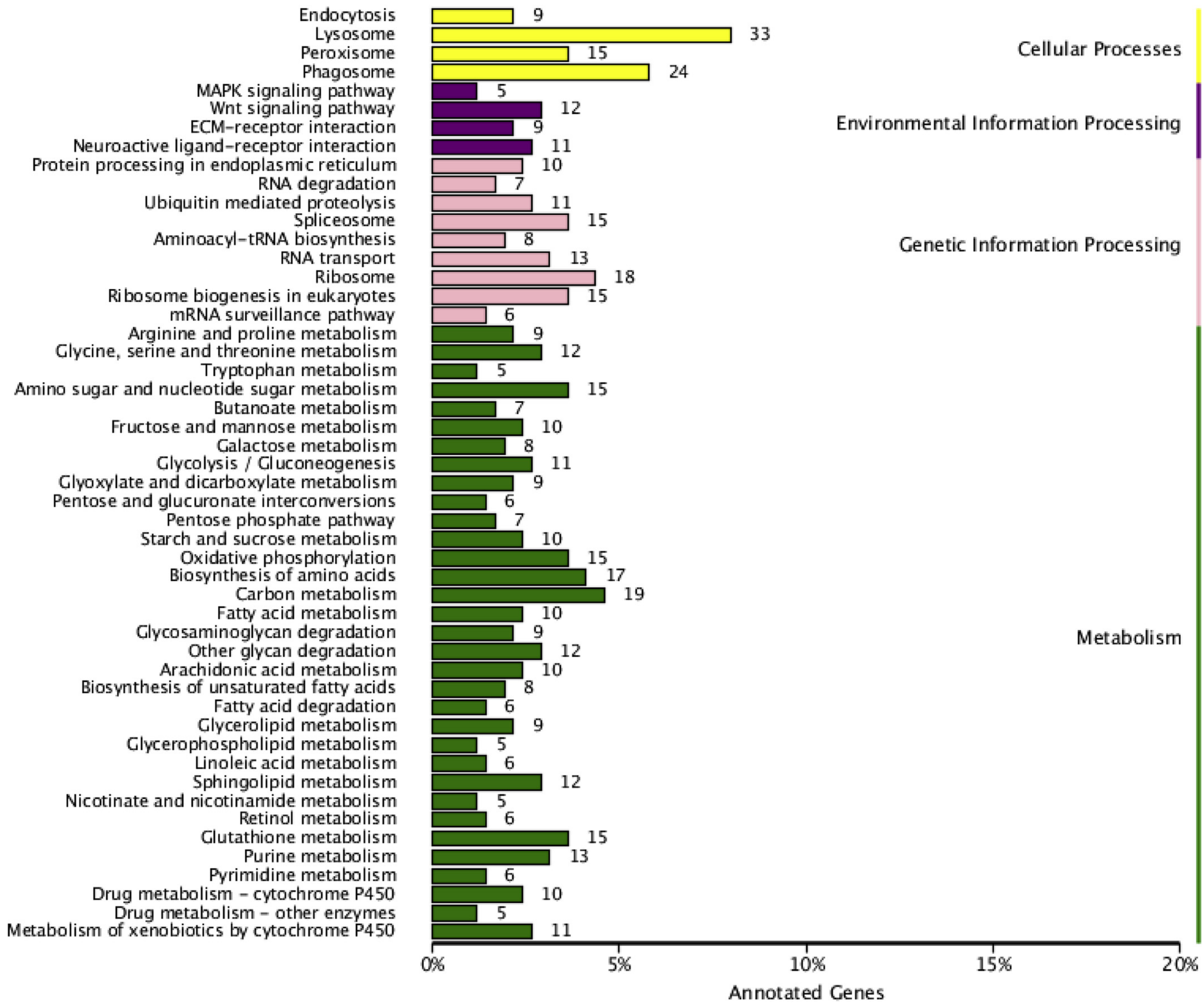


**Fig. 6.** KEGG annotation of assembled unigenes. The X-axis corresponds to the percentage of the number of genes in this pathway accounting for the total number of annotated genes. The Y-axis represents the name of pathway.

The KEGG database is a resource that is used to understand high-level functions of biological systems and to integrate the data in genomics, chemical molecules, and biochemical systems, such as pathway, drugs, disease, genes, and genome [40]. A total of 696 unigenes were assigned into 179 known pathways; the largest group was "lysosome", which plays a vital role in normal cell processes [41–43], containing 33 unigenes, followed by "phagosome" (24), "carbon metabolism" (19), and "ribosome" (18). The impairment caused by lysosomal dysfunctional leads to decreased clearance of damaged organelles and toxic macromolecules [44]. The 179 pathways were divided into four categories: "cellular processes", "environmental information processing", "genetic information processing", and "metabolism" (Fig. 6). Within the "cellular processes" category, "lysosome" (33, 4.74%) and "phagosome" (24, 3.45%) were the most common subcategories. In the "metabolism" category, "carbon metabolism" (19, 2.73%) was the most abundant subcategory. Within the "environmental information processing" category, "wnt signaling pathway" (12, 1.72%) was the most common subcategory. The majority of genes enriched in the "genetic information processing" category were involved in the "ribosome" (18, 2.59%) subcategory.

## 4. Conclusion

In conclusion, here we provide a detailed analysis of the transcriptome profile of hepatopancreas tissue from *P. clarkii* challenged with PGN. A total of 48,661 unigenes were identified and functionally annotated. When investigating the changes in *P. clarkii* after challenge with PGN, 2522 significantly DEGs were identified: 765 genes were up-regulated and 1757 were down-regulated. Among these, 954 immune-related unigenes were identified. A large number of genes and pathways involved in immune responses were identified and functionally annotated. The present study extends our understanding of the immune responses of *P. clarkii* to PGN challenge, and provides insights into the immune system and defense mechanisms activated in the hepatopancreas of *P. clarkii*.

## Acknowledgements

This work was supported by the Natural Science Foundation of Jiangsu Province (BK20160444), the National Natural Science Foundation of China (31640074), the Scientific and Technological Innovation Special Project for Seed and Seedling of Wenzhou Science &

Technology Bureau (Z20170014), the Ph.D. programs in Wenzhou Medical University (QTJ16021), the Opening Project of Zhejiang Provincial Top Key Discipline of Pharmaceutical Sciences (201721), Zhejiang Provincial Natural Science Foundation of China (LY19B020012 and LY19H160015), and sponsored by Qing Lan Project of Jiangsu Province. The authors declare no competing interests.

## References


[1] C. Manfrin, M. Tom, M.G. De, M. Gerdol, P.G. Giulianini, A. Pallavicini, The eyestalk transcriptome of red swamp crayfish *Procambarus clarkii*, Gene 557 (2015) 28–34.

[2] Y.B. Xu, J.Y. Shi, W.J. Hao, T. Xiang, H.F. Zhou, W. Wang, Q.G. Meng, Z.F. Ding, iTRAQ-based quantitative proteomic analysis of *Procambarus clakii* hemocytes during *Spiroplasma eriocheiris* infection, Fish Shellfish Immunol. 77 (2018) 438–444.

[3] R. Willmann, H.M. Lajunen, G. Erbs, M.A. Newman, D. Kolb, K. Tsuda, F. Katagiri, J. Fliegmann, J.J. Bono, J.V. Cullimore, A.K. Jehle, F. Götz, K. Kulik, A. Molinaro, V. Lipka, A.A. Gust, T.T. Nürnberger, Arabidopsis lysin-motif proteins LYM1 LYM3CERK1 mediate bacterial peptidoglycan sensing and immunity to bacterial infection, Proc. Natl. Acad. Sci. U. S. A 108 (2011) 19824–19829.

[4] J. Yan, C.Q. Zhang, Y. Zhang, K.L. Li, L.X. Xu, L.B.L. Guo, Y. Kong, L.J. Feng, Characterization and comparative analyses of two amphioxus intelectins involved in the innate immune response, Fish Shellfish Immunol. 34 (2013) 1139–1146.

[5] X.S. Li, G.B. Wang, Y. Sun, W. Liu, Y.Z. He, F.C. Wang, Y.R. Jiang, L. Qin, Transcriptome analysis of the midgut of the Chinese oak silkworm *Antheraea pernyi* infected with *Antheraea pernyi* nucleopolyhedrovirus, PLoS One 11 (2016) e0165959.

[6] K.A. Cloud-hansen, S.B. Peterson, E.V. Stab, Breaching the great wall: peptidoglycan and microbial interactions, [J] Nat Rev Microb 9 (2004) 710–716.

[7] M. Cerasuolo, On the influence of diffusion on the competition between bacteria and innate immune system of invertebrates, Ricerche mat 59 (2010) 165–185.

[8] S. Iwanaga, B.L. Lee, Recent advances in the innate immunity of invertebrate animals, J. Biochem. Mol. Biol. Evol. 38 (2005) 128–150.

[9] S. Jensen, A.R. Thomsen, Sensing of RNA viruses: a review of innate immune receptors involved in recognizing RNA virus invasion, J. Virol. 86 (2012) 2900–2910.

[10] K. Takeda, S. Akira, Toll-like receptors in innate immunity, Int. Immunol. 17 (2005) 1–14.

[11] S. Akira, Toll-like receptors in innate immunity, Adv. Immunol. 78 (2001) 1–56.

[12] Z. Wang, M. Gerstein, M. Snyder, RNA-Seq: a revolutionary tool for transcriptomics, Nat. Rev. Genet. 10 (2009) 57–63.

[13] M.G. Grabher, B.J. Haas, M. Yassour, Full length transcriptome assembly from RNA Seq data without a reference genome, Nat. Biotechnol. 29 (2011) 644–652.

[14] Y.B. Xu, J.Y. Shi, W.J. Hao, T. Xiang, H.F. Zhou, W. Wang, Q.G. Meng, Z.F. Ding, iTRAQ-based quantitative proteomic analysis of *Procambarus clarkii* hemocytes during *Spiroplasma eriocheiris* infection, Fish Shellfish Immunol. 77 (2018) 438–444.

[15] K.R. Bi, H. Huang, W. Gu, J.H. Wang, W. Wang, Phylogenetic analysis of Spiroplasmas from three freshwater crustaceans (*Eriocheir sinensis, Procambarus clarkii* and *Penaeus vannamei*) in China, J. Invertebr. Pathol. 99 (2008) 57–65.

[16] Z.F. Ding, K.R. Bi, T. Wu, W. Gu, W. Wang, J.X. Chen, A simple PCR method for the detection of pathogenic spiroplasmas in crustaceans and environmental samples, Aquaculture 265 (2007) 49–54.

[17] X.G. Du, Y.K. Li, D. Li, F.L. Lian, S.Y. Yang, J.Y. Wu, H.M. Liu, G.X. Bu, F.Y. Meng, X.H. Cao, X.Y. Zeng, H.Y. Zhang, Z.Y. Chen, Transcriptome profiling of spleen provides insights into the antiviral mechanism in *Schizothorax prenanti* after poly (I: C) challenge, Fish Shellfish Immunol. 62 (2017) 13–23.

[18] R.L. Tatusov, M.Y. Galperin, D.A. Natale, E.V. Koonin, The COG database: a tool for genome-scale analysis of protein functions and evolution, Nucleic Acids Res. 28 (2000) 33–36.

[19] J. Huerta-Cepas, D. Szklarczyk, K. Forslund, H. Cook, D. Heller, M.C. Walter, T. Rattei, D.R. Mende, S. Sunagawa, M. Kuhn, L.J. Jensen, C.V. Mering, P. Bork, eggNOG 4.5: a hierarchical orthology framework with improved functional annotations for eukaryotic, prokaryotic and viral sequences, Nucleic Acids Res. 44 (2015) D283–D293.

[20] D. Szklarczyk, A. Franceschini, M. Kuhn, M. Simonovic, A. Roth, P. Minguez, T. Doerks, M. Stark, J. Muller, P. Bork, L.J. Jensen, C.V. Mering, The STRING database in 2011: functional interaction networks of proteins, globally integrated and scored, Nucleic Acids Res. 39 (2010) D561–D568.

[21] C. Trapnell, B.A. Williams, G. Pertea, A. Mortazavi, G. Kwan, M.J. Baren, S.L. Salzberg, B.J. Wold, L. Pachter, Transcript assembly and abundance estimation from RNA-Seq reveals thousands of new transcripts and switching among isoforms, Nat. Biotechnol. 28 (2010) 511–515.

[22] Y.Y. Deng, J.Q. Li, S.F. Wu, Integrated nr database in protein annotation system and its localization, Computer Engineering Italic 32 (2006) 71–74.

[23] Z.Z. Xin, Q.N. Liu, Y. Liu, D.Z. Zhang, Z.F. Wang, H.B. Zhang, B.M. Ge, C.L. Zhou, X.Y. Chai, B.P. Tang, Transcriptome-wide identification of differentially expressed genes in Chinese oak silkworm *Antheraea pernyi* in response to lead challenge, J. Agric. Food Chem. 65 (2017) 9305–9314.

[24] X. Mao, T. Cai, J.G. Olyarchuk, L. Wei, Automated genome annotation and pathway identification using the KEGG Orthology (KO) as a controlled vocabulary, Bioinformatics 21 (2005) 3787–3793.

[25] J. Seong, S.W. Kang, B.B. Patnaik, S.Y. Park, H.J. Hwang, J.M. Chung, D.K. Song, M.Y. Noh, S.H. Park, G.J. Jeon, H.S. Kong, S. Kim, U.W. Hwang, H.S. Park, Y.S. Han, Y.S. Lee, Transcriptome analysis of the tadpole shrimp (*Triops longicaudatus*) by illumina paired-end sequencing: assembly, annotation, and marker discovery, Genes 7 (2016) 114.

[26] M. Kanehisa, M. Araki, S. Goto, M. Hattori, M. Hirakawa, M. Itoh, T. Katayama, S. Kawashima, S. Okuda, T. Tokimatsu, Y. Yamanishi, KEGG for linking genomes to life and the environment, Nucleic Acids Res. 36 (2008) D480–D484.

[27] H.N. Wu, Y.Q. Zhang, W.B. Zhang, X.W. Pei, C. Zhang, S. Jia, W.M. Li, Transcriptomic analysis of the primary roots of *Alhagi sparsifolia* in response to water stress, PLoS One 10 (2015) e0120791.

[28] M.D. Young, M.J. Wakefield, G.K. Smyth, A. Oshlack, Gene ontology analysis for RNA-Seq: accounting for selection bias, Genome Biol. 11 (2010) R14.

[29] A. Conesa, S. Götz, J.M. Garcia-Gomez, J. Terol, M. Talon, M. Robles, Blast2GO: a universal tool for annotation, visualization and analysis in functional genomics research, Bioinformatics 21 (2005) 3674–3676.

[30] C. Scheidt-Nave, P. Kamtsiuris, A. Gößwald, H. Hölling, M. Lange, M.A. Busch, S. Dahm, R. Dölle, U. Ellert, J. Fuchs, U. Hapke, C. Heidemann, H. Knopf, D. Laussmann, G.B.M. Mensink, German health interview and examination survey for adults (DEGS) - design, objectives and implementation of the first data collection wave, BMC Publ. Health 12 (2012) 730.

[31] Y.Y. Wang, R.Y. Chen, Y.W. Hao, H.C. Liu, S.W. Song, G.W. Sun, Transcriptome analysis reveals differentially expressed genes (DEGs) related to lettuce (*Lactuca sativa*) treated by TiO2/ZnO nanoparticles, Plant Growth Regul. 83 (2017) 13–25.

[32] Y. Liu, Z.Z. Xin, D.Z. Zhang, X.Y. Zhu, Y. W, L. Chen, B.P. Tang, C.L. Zhou, X.Y. Chai, J.W. Tian, Q.N. Liu, De novo transcriptome assembly and analysis of differential gene expression following peptidoglycan (PGN) challenge in *Antheraea pernyi*, Int. J. Biol. Macromol. 112 (2018) 1199–1207.

[33] F.L. Zhou, K.M. Zhou, J.H. Huang, Q.B. Yang, S. Jiang, L.H. Qiu, L.S. Yang, S.G. Jiang, Characterization and expression analysis of a chitinase gene (PmChi-5) from black tiger shrimp (*Penaeus monodon*) under pathogens infection and ambient ammonia-N stress, Fish Shellfish Immunol. 72 (2018) 117–123.

[34] M. Rinaudo, Chitin and Chitosan — properties and applications, ChemInform 31 (2007) 603–632.

[35] Y.H. Zhang, S.Z. Feng, J. Chen, C.B. Qin, H.R. Lin, W.S. Li, Stimulatory effects of chitinase on growth and immune defense of orange-spotted grouper (*Epinephelus coioides*), Fish Shellfish Immunol. 32 (2012) 844–854.

[36] W.D. Fu, F.J. Zhang, M.F. Liao, M.H. Liu, B. Zheng, H.C. Yang, M.J. Zhong, Molecular cloning and expression analysis of a cytosolic heat shock protein 70 gene from mud crab *Scylla serrata*, Fish Shellfish Immunol. 32 (2012) 844–854.

[37] M.K. Chaurasia, F. Nizam, G. Ravichandran, M.V. Arasu, N.A. Al-Dhabi, A. Arshad, P. Elumalai, J. Arockiaraj, Molecular importance of prawn large heat shock proteins 60, 70 and 90, Fish Shellfish Immunol. 48 (2016) 228–238.

[38] L. Lagos, J.I. Tandberg, M.I. Becker, H.C. Winther-Larsen, Immunomodulatory properties of *Concholepas concholepas* hemocyanin against francisellosis in a zebrafish model, Fish Shellfish Immunol. 67 (2017) 571–574.

[39] P.K. Yang, D.F. Yao, J.J. Aweya, F. Wang, P. Ning, S.K. Li, H.Y. Ma, Y.L. Zhang, c-Jun regulates the promoter of small subunit hemocyanin gene of *Litopenaeus vannamei*, Fish Shellfish Immunol. 84 (2019) 639–647.

[40] P.A. Zhang, H.J. Wu, H. Xue, X.R. Ju, W. Song, Q.L. Zhang, M.L. Yuan, Characterization of transcriptome in the Indian meal moth *Plodia interpunctella* (Lepidoptera: Pyralidae) and gene expression analysis during developmental stages, Gene 622 (2017) 29–41.

[41] Kameswaran Surendran, Seasson P. Vitiello, David A. Pearce, Lysosome dysfunction in the pathogenesis of kidney diseases, Pediatr. Nephrol. 29 (2014) 2253–2261.

[42] S.S.K. Durairajan, Y.Y. Huang, L.L. Chen, J.X. Song, L.F. Liu, M. Li, Corynox ne isomers decrease levels of amyloid-β peptide and amyloid-β precursor protein by promoting autophagy and lysosome biogenesis, Mol. Neurodegener. 8 (2013) P16.

[43] T. Shiraishi, K. Tsunematsu, T. Matsushima, M. Sasaki, S. Suzuki, The studies in alterations of lysosomal enzymes in hepatic disorders — with special reference to the application of the lysosome stabilizer to the treatment of liver disease, Gastroenterol. Jpn. 3 (1968) 309.

[44] Y. Yin, E. Li, G.S. Hong, Q. Yan, L.M. Foley, L.A. Andrzejczuk, I.Y. Attarwala, T.K. Hitchens, K. Kiselyov, C.E. Dixon, D.D. Sun, Effects of DHA on hippocampal autophagy and lysosome function after traumatic brain injury, Mol. Neurobiol. 55 (2018) 2454–2470.